



**Aalborg Universitet**

**AALBORG UNIVERSITY**  
DENMARK

## **Retention of microplastics in sediments of urban and highwaystormwater retention ponds**

Liu, Fan; Vianello, Alvisè; Vollertsen, Jes

*Published in:*  
Environmental Pollution

*DOI (link to publication from Publisher):*  
[10.1016/j.envpol.2019.113335](https://doi.org/10.1016/j.envpol.2019.113335)

*Creative Commons License*  
CC BY 4.0

*Publication date:*  
2019

*Document Version*  
Publisher's PDF, also known as Version of record

[Link to publication from Aalborg University](#)

*Citation for published version (APA):*  
Liu, F., Vianello, A., & Vollertsen, J. (2019). Retention of microplastics in sediments of urban and highwaystormwater retention ponds. *Environmental Pollution*, 255, [113335].  
<https://doi.org/10.1016/j.envpol.2019.113335>

### **General rights**

Copyright and moral rights for the publications made accessible in the public portal are retained by the authors and/or other copyright owners and it is a condition of accessing publications that users recognise and abide by the legal requirements associated with these rights.

- ? Users may download and print one copy of any publication from the public portal for the purpose of private study or research.
- ? You may not further distribute the material or use it for any profit-making activity or commercial gain
- ? You may freely distribute the URL identifying the publication in the public portal ?

### **Take down policy**

If you believe that this document breaches copyright please contact us at [vbn@aub.aau.dk](mailto:vbn@aub.aau.dk) providing details, and we will remove access to the work immediately and investigate your claim.



# Retention of microplastics in sediments of urban and highway stormwater retention ponds<sup>☆</sup>

Fan Liu<sup>\*</sup>, Alvis Vianello, Jes Vollertsen

Department of Civil Engineering, Aalborg University, Thomas Manns Vej 23, 9220 Aalborg, Denmark



## ARTICLE INFO

### Article history:

Received 28 May 2019

Received in revised form

5 September 2019

Accepted 30 September 2019

Available online 30 September 2019

### Keywords:

Microplastics

Sediments

Stormwater retention ponds

Urban runoff

Freshwater

## ABSTRACT

Urban and highway surfaces discharge polluted runoff during storm events. To mitigate environmental risks, stormwater retention ponds are commonly constructed to treat the runoff water. This study is the first to quantify the retention of microplastics in the sediments of such ponds. It applied state-of-art FTIR-methods to analyse the composition, size, shape, and mass of microplastics in the range 10–2000  $\mu\text{m}$ . Seven ponds serving four land uses were investigated, and the results are related to catchment characteristics, sediment organic matter content, and hydraulic loading. We have not found a correlation between the microplastics abundance, polymer composition, size distribution and the land use in the catchment, as well as the sediment organic matter content. Both the highest (127,986 items  $\text{kg}^{-1}$ ; 28,732  $\mu\text{g kg}^{-1}$ ) and the lowest (1511 items  $\text{kg}^{-1}$ ; 115  $\mu\text{g kg}^{-1}$ ) accumulation of microplastics were found in the sediments of ponds serving industrial areas. There was, however, a correlation to the hydraulic loading of the ponds, where the sediments of the highest-loaded ponds held the most microplastics. This study shows that sediments in stormwater retention ponds can trap some of the microplastics and prevent them from being transported downstream. These systems need to be considered when assessing the fate of microplastics from urban and highway areas.

© 2019 The Authors. Published by Elsevier Ltd. This is an open access article under the CC BY license (<http://creativecommons.org/licenses/by/4.0/>).

## 1. Introduction

Plastic has become ubiquitous in the environment due to the continuous increase in its production (PlasticsEurope, 2018); and its inherent resistance to degradation (Koelmans et al., 2019; Windsor et al., 2019). Currently, an estimated 4.8–12.7 million metric tons enter the oceans annually (Jambeck et al., 2015). The role of microplastics (MPs) as part of plastic pollution has recently received scientific, public, and political attention. Compared with larger plastic debris, MPs have a higher surface-to-volume ratio, leading to an increased potential to release additives and adsorb organic chemicals (Velzeboer et al., 2014; Zhan et al., 2017; Hahladakis et al., 2018). Investigation of MPs in freshwater and terrestrial environments began quite recently (Eriksen et al., 2013). Since then, studies on freshwater-related MPs began to emerge, and wastewater treatment plants (WWTP) have been well-documented as point sources (McCormick et al., 2014; Talvitie et al., 2017; Simon et al., 2018). In addition, urban and highway

stormwater runoff is known to be a land-to-sea pathway for MPs, although it has received substantially less attention in terms of experimental studies (Auta et al., 2017). One of the few such studies shows that MP concentrations in urban and highway runoff could be related to how land in the drained catchment is used (Liu et al., 2019b).

Before discharging the runoff, an increasing portion of stormwater runoff is treated by sustainable stormwater management technologies such as stormwater retention ponds (Hvitved-Jacobsen et al., 2010). The runoff is drained into the pond and held from days to weeks before discharge, allowing pollution removal processes to occur. Sorption and degradation are the dominant processes for eliminating soluble pollutants like biocides and pharmaceuticals (Minelgaite et al., 2017; Liu et al., 2019a). For particulate materials, sedimentation and deposition are the main removal mechanisms. For these processes, the size, shape, and density of particles are critical parameters, as they affect directly the particle movement in water and determine their final deposition (Hvitved-Jacobsen et al., 2010). For synthetic particles, the formation of biofilm on the surface can further promote the particle deposition, which makes sedimentation occur even for low-density polymers (Rummel et al., 2017; Harrison et al., 2018). With their

<sup>☆</sup> This paper has been recommended for acceptance by Dr. Sarah Harmon.

<sup>\*</sup> Corresponding author.

E-mail address: [fl@civil.aau.dk](mailto:fl@civil.aau.dk) (F. Liu).

retention, sediments can largely reduce the mobility of MPs in water, hence decrease the transportation to another water environment. However, accumulation in the sediments protects MPs from solar UV light, which leads to the deposited MPs becoming less degraded compared to those subjected to direct UV exposure (Andrady, 2017; Da Costa et al., 2018). Therefore, retained MPs can accumulate in the sediments over the years, until the sediments eventually are removed, de-watered, and sent to a soil treatment facility for further processing (Hvitved-Jacobsen et al., 2010).

MPs found in sediments, typically collected as a grab sample by various means such as Van Veen grabs (Di and Wang, 2018; Haave et al., 2019), shovels (Wang et al., 2017), spatulas (Abidli et al., 2018), and sediment corers (Vaughan et al., 2017), can be understood to comprise a long-term average of MPs. The analytical methods for MPs identification and quantification are less straightforward, and the applied approaches vary substantially (Van Cauwenberghe et al., 2015; Cabernard et al., 2018; Hartmann et al., 2019). Over the later years, focal plane array (FPA)-based micro-Fourier-Transform Infrared ( $\mu$ FTIR) microscopy combined with automated image analysis has proven to be a comparatively reliable method for MP quantification. This approach reduces the bias caused by manual particle sorting and allows for robust quantification of particles down to sizes of roughly 10  $\mu$ m (Primpke et al., 2017; Simon et al., 2018; Liu et al., 2019b).

The objective of this study was to quantify the retention of MPs, in the range 10–2000  $\mu$ m, in the sediments of stormwater retention ponds. FPA-based  $\mu$ FTIR imaging was used to quantify MPs below 500  $\mu$ m, and attenuated total reflectance (ATR)-based FTIR was used to identify larger particles. We hypothesised that the accumulation of MPs in pond sediments would correlate with catchment characteristics, sediment characteristics, and hydraulic loading. Seven ponds with drainage areas covering four land use types were chosen for evaluation.

## 2. Material and methods

### 2.1. Sampling

Sediments were collected from seven stormwater retention ponds in Denmark in March and April 2017. The ponds received stormwater runoff from catchments of different land use. Three served residential areas (R1, R2, R3), two served industrial areas (I1, I2), one had a commercial catchment (C1), and one received runoff from a highway (H1). Six of the ponds were around 10 years old. One pond was much older, but had its sediments dredged some 10–15 years ago (Table 1).

The sampling was done in dry weather, with an antecedent dry

weather period of at least two days. Samples were taken at 1 m water depth using a Van Veen bottom grab sampler and stored in 1 L glass jars. The jars were closed with non-sealing glass lids. Only the top 5 cm of the sediments were collected from each grab. At 1 m water depth, deposited sediments are not prone to wind-induced re-suspension (Bentzen et al., 2009) and sediment accumulation rates can be expected to range between 0.7 and 1.6  $\text{cm y}^{-1}$  (Damrat et al., 2013; Szymkiewicz and Zalewska, 2014). Hence the samples are expected to represent the long-term average of approximately 3–7 years of sediment accumulation. For each pond, samples were collected the same day from three randomly locations; sediments from the same pond were combined and analysed as one sample (Wang et al., 2018). A minimum of 3 L of sediments was collected from each pond. All samples were immediately transferred to the laboratory and stored at 5 °C until analysis. Sediment organic matter content was determined by the weight loss on ignition (LOI): the dried sediments were placed into a muffle furnace and heated to 550 °C for 4 h (Hurley et al., 2018).

### 2.2. Sample processing

The isolation of MPs from the sediments followed a method derived from Masura et al. (2015) and Mintenig et al. (2017). First, particles larger than 2 mm were removed from the 3 L of the wet sediments by wet-sieving, using a 2 mm sieve (Retsch GmH, Germany). The wet-sieving used 1.2  $\mu$ m GF filtered Milli-Q water (47 mm in diameter, Whatman), and the sieved sample was collected in 5 L glass beakers. To reduce the large water volume that resulted from the wet-sieving, the collected samples were settled for one week, after which the supernatant was filtered through a 10  $\mu$ m stainless steel mesh (47 mm in diameter, laser-cut from larger filter sheets, Filtertek A/S, Denmark). The filter was then collected in a glass beaker containing 20–30 mL Milli-Q water and sonicated for 15 min. Particles remaining on the filter were carefully flushed into the solution and transferred back into the 5 L beaker containing the settled sediments.

Sediments contain aggregates of organic matter and the fine inorganic particles which can trap MPs. This could reduce the extraction efficiency of the density separation as such agglomerated particles can have densities close to sand and clay, and hence lead to a loss of MPs (Kooi et al., 2018). To avoid this bias, the sediments went through a pre-oxidation designed to reduce the organic matter content and open up the matrix before the density separation. Peroxide-based treatment has proven efficient for organic matter removal, and a concentration of 30%  $\text{H}_2\text{O}_2$  has commonly been used for such treatment (Hurley et al., 2018). However, prior to processing the pond samples, initial tests on the

**Table 1**  
Overview of stormwater ponds, their catchments, and the organic matter content of the sampled sediments.

Site	City	Coordinate (N, E)	Hydraulic loading: catchment impervious area per pond surface area ( $\text{m}^2/\text{m}^2$ )	Catchment type	Organic matter (% dry weight)
R1	Silkeborg	(56° 11' 39.8", 9° 32' 57.9")	71000/4000	Residential with single-family houses and part of an orbital road. Constructed: 2008	1.01
R2	Aarhus	(56° 10' 18.4", 10° 05' 49.9")	426000/11880	Residential with single family houses. Constructed: 2005	2.10
R3	Aarhus	(56° 10' 18.4", 10° 06' 22.6")	466000/11900	Residential with single family houses. Constructed: 2005	3.26
I1	Aarhus	(56° 10' 49.0", 10° 07' 58.4")	109000/7460	Light industry. Constructed: 2007	3.61
I2	Viborg	(56° 28' 29.3", 9° 24' 43.3")	698000/6500	Light industry, commerce, do-it-yourself shops. Constructed before 1995. Dredged for sediments approx. 10–15 years before sampling	8.96
C1	Aarhus	(56° 08' 41.8", 10° 08' 12.2")	190000/6050	Commercial (shopping centre), some residential use. Constructed: 2008	1.13
H1	Aarhus	(56° 13' 13.9", 10° 07' 43.5")	48000/5540	Highway. Constructed: 2009	2.30

same matrix had shown that the use of 30% H<sub>2</sub>O<sub>2</sub> can lead to an uncontrolled exothermic reaction and gas production for storm-water pond sediments, which may potentially cause loss of MPs. Hence the sediment samples were divided into several smaller batches, which each underwent oxidation at a lower peroxide concentration. Briefly, approx. 50 g of wet sediments were sub-sampled from the sieved sediments and placed in a 2 L glass beaker. The beaker was filled with 200 mL Milli-Q water before adding 30 mL of 30% H<sub>2</sub>O<sub>2</sub> (achieving a final H<sub>2</sub>O<sub>2</sub> concentration of 4%), thus achieving a diluted peroxide solution. The reactor was kept at 50 °C by placing it on a heating plate and gently stirring it. The temperature was monitored and, in case the solution overheated due to the exothermic oxidation reaction, the beaker was placed in an ice-water bath until the thermal reaction slowed down. The oxidation was continued by adding another 30 mL of 30% H<sub>2</sub>O<sub>2</sub> every 24 h, until no foaming was observed when adding peroxide. The pre-oxidized sediments were transferred onto a glass dish and dried in an oven at 50 °C. This procedure was repeated until all 3 L of sediments had been processed. The dried sediments were combined and subjected to further oxidation with 15% H<sub>2</sub>O<sub>2</sub> on a heating plate (50 °C) for 7 days. Temperature was monitored during the oxidation. Subsequently the sediments were oven-dried at 50 °C.

A sub-sample of 200 g dry sediments underwent density separation using 1.5 L of zinc chloride solution (1.97 g cm<sup>-3</sup>), and the MPs abundance was quantified based on this dry weight. The separation was performed twice in a 2 L glass funnel. In the first separation, the mixed solution was aerated with dry and dust-free compressed air for 1 h and allowed to settle for 5 h. The settled particles were drained off through the bottom of the funnel. In the second separation, the solution was aerated for 30 min and left to settle overnight, after which the settled particles were again drained off. The remaining liquid was filtered through a 10 µm stainless steel filter. The pre-oxidation – intended to open up the matrix prior to density separation – was insufficient to remove all organic matter. The collected particles hence underwent a Fenton reaction by adding 146 mL 50% H<sub>2</sub>O<sub>2</sub>, 63 mL of 0.1 M FeSO<sub>4</sub>, and 65 mL of 0.1 M NaOH (Simon et al., 2018). The reaction was kept at 15–19 °C by putting the reactor on ice. After the reaction had slowed down sufficiently, the reactors were left for 2 days at room temperature. After that, the liquid was filtered through a 500 µm stainless steel sieve, followed by a 10 µm steel filter. The particles remaining on the sieve (500–2000 µm) were collected, dried at 50 °C, and analysed with ATR-FTIR. Particles on the steel filter (10–500 µm) were collected into HPLC grade ethanol by ultrasonication, then transferred into a glass vial and evaporated by nitrogen (N5.0) until dry. Finally, 5 mL of 50% ethanol was added to the vial.

### 2.3. MP identification and quantification

MPs <500 µm were analysed as described in Liu et al. (2019b) and Simon et al. (2018), yielding major dimension, minor dimension, and estimated mass for each particle. Briefly, a sub-sample of the 5 mL particle concentrate was deposited on a zinc selenide window, where a compression cell (Pike Technologies, USA) was used to restrict the surface to a diameter of 10 mm. The window was dried at 55 °C and scanned at a pixel resolution of 5.5 µm (µFTIR imaging), using a Cary 620 FTIR microscope coupled with a Cary 670 IR spectrometer (Agilent Technologies). The microscope used a 15x Cassegrain objective and a 128 × 128 Mercury–Cadmium–Telluride (MCT) FPA detector. The resulting IR maps were analysed using MPhunter (Liu et al., 2019b). The wavenumber range was analysed using 900–3750 cm<sup>-1</sup>. The library used by MPhunter contained 113 reference spectra, organized into 29 material groups:

ABS (acrylonitrile butadiene styrene), acrylic, acrylic paints, alkyd, aramid, cellulose acetate, diene elastomer, EPDM (ethylene propylene diene monomers), epoxy, EVA (ethylene vinyl acetate), PA (polyamide), PAN Acrylic fibre (polyacrylonitrile), PE (polyethylene), Pebax®, PEG (polyethylene glycol), phenoxy resin, PLA (polylactic acid), polycarbonate, polyester, POM (polyoxymethylene), PP (polypropylene), PS (polystyrene), PTFE (polytetrafluoroethylene), PU (polyurethane), PU paints (polyurethane paints), PVA (polyvinyl alcohol), PVAC (polyvinyl acetate), PVC (polyvinyl chloride), SAN (styrene acrylonitrile), SBR (styrene butadiene rubber), and vinyl copolymer. In addition, to reduce the risk of false-positive detections, the database contained cellulose and proteinaceous material. Three replicates from the 5 mL particle concentrate were sub-sampled, deposited, scanned by µFTIR, and analysed by MPhunter. The results of the 3 scans were combined and interpreted as the final result (Liu et al., 2019b).

MPs >500 µm were visually sorted with ultra-fine micro forceps under a stereomicroscope (Stereo Discovery V8, Zeiss, Oberkochen, Germany). The chemical composition of each potential MP particle was confirmed with ATR-FTIR (Cary 630 FTIR Spectrometer, Agilent Technologies, equipped with a single reflection diamond ATR crystal). Spectra were collected over the wavenumber range 650–4000 cm<sup>-1</sup>. The particles were analysed by 32 co-added scans, with a background correction of 64 co-added scans and a resolution of 8 cm<sup>-1</sup>. The spectra of samples were analysed using OMNIC 8.3 software (Thermo Fisher Scientific, Madison, WI, USA) software by comparing them to the several reference polymer libraries, including the spectral library developed by JPI-OCEANS, BASEMAN (Primpke et al., 2018). The sample's polymer type was determined by a combination of the best-fitted spectra and the expertise of the operator on interpreting polymer IR spectra. Each identified particle was measured in both its major and minor dimensions, using the stereomicroscope's software (ZEN Core, Zeiss, Oberkochen, Germany). The mass of the particle was estimated based on the same assumptions used for particles <500 µm: first, the volume was estimated while assuming that the thickness was 67% of the minor dimension and that the particle had an ellipsoid shape. The mass was estimated from the volume and density of the polymer material. Car tyre rubber could not be identified by the FTIR techniques, as it contains carbon black as a filler, which absorbs light throughout the infrared region (Kole et al., 2017).

### 2.4. Experimental quality control

To minimize contamination during sample processing, only glass, stainless steel, and PTFE-coated labware was used. PTFE was excluded in this study, as it has a density of 2.2 g cm<sup>-3</sup>, and these particles hence would be drained off with the inorganics in the density separation. All labware was flushed with Milli-Q water beforehand and covered with a watch glass or aluminium foil immediately after each treatment step. Sieves and steel filters were muffled at 500 °C. Cotton lab coats were worn during all process steps. Samples were processed inside a fume hood whenever possible, and the air of the FTIR room was continuously filtered by an air treatment device (Dustbox® Hochleistungsluftreiniger, Germany) with a HEPA filter (H14, 7.5 m<sup>2</sup>). All open containers were covered with watching glass or aluminium foil. Even so, contamination could still occur from cloth, lab dust, etc. (Woodall et al., 2014; Dris et al., 2017). Hence, the background contamination from the sample processing was assessed by use of three blanks. Washed and muffled (500 °C) sand of 75–1000 µm (Baskarp Sand No. 15) was used. The blanks went through the same processes described for the sediment samples.

Recovery was tested in triplicate for the density separation step by spiking 300 items of red 100 µm PS beads (Sigma-Aldrich,

product no. 56969) into 200 g the muffled sand (Fig. S1). The spiked sand went through the separation following the steps described above, and the 10  $\mu\text{m}$  stainless steel filters were investigated under a stereomicroscope and the beads counted.

## 2.5. Statistical analysis

The Shapiro-Wilk normality test was used to test the normality of datasets. All statistical analysis was performed in R (v3.5.1), and the significance level in all cases was set to 0.05.

## 3. Results

### 3.1. Background contamination and recovery

For each of the three blank samples, a sub-sample of 400  $\mu\text{L}$  was deposited and scanned. Only five MPs were found in total in the blanks. All were of PE with a summed estimated mass of 17.5 ng. This corresponds to 20.8 items and 72.9 ng per sample processing. Compared to some other studies, the slightly higher MP number in the blanks could be explained by the different MP identification and quantification method applied. For instance, Yang et al. (2019) and Allen et al. (2019) both found < 10 items in the procedural blanks. But they used manual sorting in their study, which could introduce human bias and lead to an underestimation of MPs especially for particles < 500  $\mu\text{m}$  (Hidalgo-Ruz et al., 2012). In the present study, all MPs found in the blanks were between 16.5  $\mu\text{m}$  and 75.1  $\mu\text{m}$ , and could easily have been missed if manual sorting had been applied instead of automated analysis. Compared to the studies applying a similar MP analysis method, the contamination in the present study was much lower. For instance, Simon et al. (2018) stated that 2110 MPs (84  $\mu\text{g}$ ) had been found, while Mintenig et al. (2017) reported that 21 particulate and 130 fibrous MPs were detected in their blanks.

Since the blank tests were conducted on muffled sand, the contamination is related to the inorganic fraction of the processed sample. As 200 g of dry sediments were processed, the contamination accounted for 104 items  $\text{kg}^{-1}$  and 0.36  $\mu\text{g kg}^{-1}$ , which corresponded to 1% and 0.02% of the average MP number and mass concentration of the field samples, respectively (Table S1). This was lower than the 6.8% reported by Su et al. (2016). Since the background contamination is subject to variation (Scheurer and Bigalke, 2018), and to avoid unknown biases and simplify data interpretation, the results were not corrected for this background contamination.

The density separation showed a recovery of  $66 \pm 5.6\%$ . For comparison, Olesen et al. (2019) found a quite similar recovery (64%) for extraction of MPs from stormwater pond sediments. It should be noted that the actual recovery rate could differ from this value. One reason is that some of the microbeads – although recovered by the separation – were covered by other materials on the filter (Fig. S1). Another reason is that microbeads probably behave differently from the polymers found in the field samples because polymer types, shapes, and size differ. Hence to avoid these unknown biases, the results were not corrected by the recovery rate.

### 3.2. MP abundance and size

Various studies have shown that MP abundance in terms of particle number increases with decreasing size (Mintenig et al., 2017; Cabernard et al., 2018; Simon et al., 2018). However, reported studies have applied different sampling methods and analytical techniques to different targeted size ranges (Hartmann et al., 2019). These differences make the reporting of MP

abundance challenging and complicate inter-study comparisons (Hartmann et al., 2019; Liu et al., 2019b). In this study we choose an upper cut-off in particle size of 2 mm as the number of large particles in the samples was low (Horton et al., 2017), and the finding of single large particles would be quite random, introducing a large bias in the mass estimate (Simon et al., 2018). The lower size limit set to 10  $\mu\text{m}$  as this was the pore size of the glitters used in the sample preparation. MP abundance was reported by the MP's major dimension, which was classed into size ranges that are commonly used in other studies (Leslie et al., 2017; Vaughan et al., 2017; Peng et al., 2018; Zhang and Liu, 2018). Five unevenly distributed fractions were used: 10–50  $\mu\text{m}$ , 50–250  $\mu\text{m}$ , 250–500  $\mu\text{m}$ , 500–1000  $\mu\text{m}$ , and 1000–2000  $\mu\text{m}$  (Fig. 1).

A total of 2232 particles were identified as MPs among all analysed samples, among which 1135 items were within the size range of 10–50  $\mu\text{m}$ , while only 5.3% (118 items) were above 250  $\mu\text{m}$  (Fig. 1A). The highest number concentration was found in the fraction of 10–50  $\mu\text{m}$  (8894 items  $\text{kg}^{-1}$ ), while the lowest was in the fraction of 500–1000  $\mu\text{m}$  (118 items  $\text{kg}^{-1}$ , Fig. 1B). In contrast, these two fractions had the lowest and highest mass concentration (43  $\mu\text{g kg}^{-1}$  and 1054  $\mu\text{g kg}^{-1}$ , respectively, Fig. 1C), which was quite expectable as number of particles increase with decreasing particle size. The accumulated particle number and mass concentration from all size classes were 17490 items  $\text{kg}^{-1}$  and 3085  $\mu\text{g kg}^{-1}$ , respectively. Comparing with other freshwater-related studies, the overall particle number concentration found was generally several orders of magnitude higher. For instance, MP concentration in river sediments from Shanghai was found to be 802 items  $\text{kg}^{-1}$  (Peng et al., 2018), while it ranged from  $178 \pm 69$  to  $544 \pm 107$  items  $\text{kg}^{-1}$  in sediments from the Beijing River littoral zone (Wang et al., 2017). Nel et al. (2017) reported that MPs were present at an overall average concentration of  $160.1 \pm 139.5$  items  $\text{kg}^{-1}$  in a South African temperate urban river system during winter.

There are several possible reasons for the differences in MPs number concentrations. One is that some studies used less dense solutions, such as NaCl and  $\text{CaCl}_2$  (1.2–1.3  $\text{g mL}^{-1}$ ), to separate MPs from the inorganics. Such density is insufficient to extract high-density polymers such as PVC or polyester (Van Cauwenberghe et al., 2015; Leslie et al., 2017; Scheurer and Bigalke, 2018). In the present study, the high-density polymers constituted 13.5% of all MPs (244 polyester and 57 PVC, Table S2). Another reason is related to the different particle cut-off size applied. This study used 10  $\mu\text{m}$  as the lower limit of detection, which is smaller than the sizes reported by most other studies. For instance, Horton et al. (2017) investigated MPs in the sediments of the River Thames (UK) and found 660 items  $\text{kg}^{-1}$  of 1–4 mm MP. A range of 18–629 items  $\text{kg}^{-1}$  of MPs was found in the Antuã River, Portugal, using 55  $\mu\text{m}$  as the cut-off size (Rodrigues et al., 2018). However, the present study showed that particles < 50  $\mu\text{m}$  constituted more than half (1135 items) of all MPs. Another difference relates to the analytical detection method. Other studies have applied manual sorting of particles under a microscope, followed by a material verification of the collected particles. The present study applied  $\mu\text{FTIR}$  imaging combined with automated MP identification, a method that minimizes false negatives and reduces human bias in the analytical procedure (Löder et al., 2017; Primpke et al., 2017). Finally, the sampled matrices do of course differ, and it cannot be expected that sediments from stormwater retention ponds should hold the same concentration of MPs as, for example, river sediments.

Compared to the few cases where mass concentrations have been reported, the mass concentrations of the present study were lower. This can be because of the vast majority of the identified MPs were small-sized particles, which had less mass contribution compared to larger particles in other studies. For instance, a Swiss floodplain was found to be contaminated by MPs at a concentration

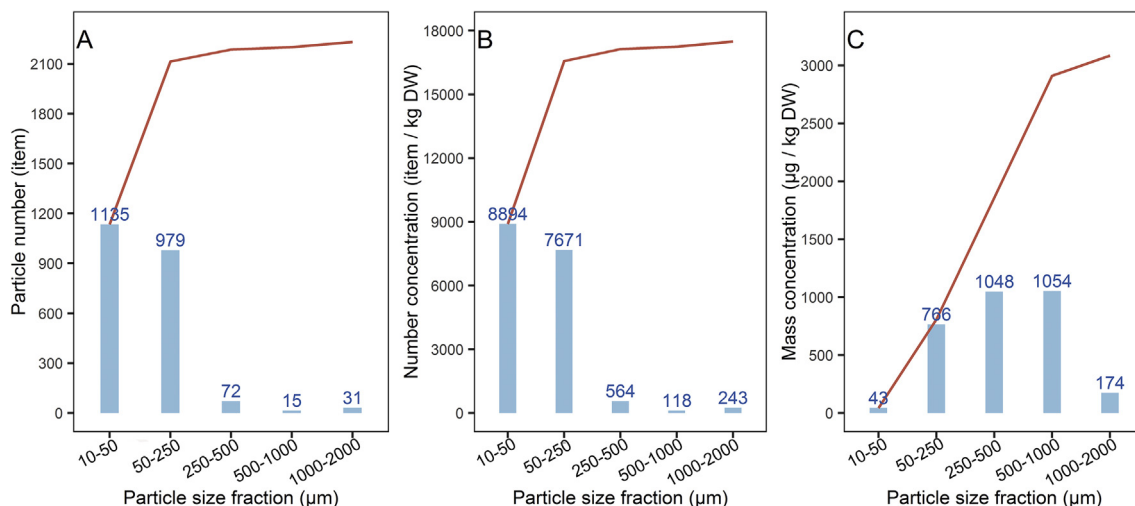


**Fig. 1.** MP abundance in the sediments of the seven ponds. (A) shows the distribution of the 2232 MP particles found; (B) the calculated number concentrations in the size bins; and (C) the calculated mass concentration. The blue bars are the abundance in each size fraction, and the red lines show the corresponding accumulated abundance. (For interpretation of the references to colour in this figure legend, the reader is referred to the Web version of this article.)

up to 55.5 mg kg<sup>-1</sup> (Scheurer and Bigalke, 2018), but the majority (88%) of the MPs were larger particles of 125–500 µm.

### 3.3. Relation between MP abundance and pond characteristics

As climate conditions at the seven sites are similar, the ratio between the impervious catchment area and the pond surface area is used as a surrogate for their specific hydraulic loading (Table 1). A positive correlation was observed between the pond hydraulic loading and the MP abundance, both in particle number (Fig. 2A) and mass concentration (Fig. 2B). Sediment's organic matter content also showed a correlation towards the MP mass concentration, but with less significance (P-value of 0.02, Fig. 2D). It should be noted that the low number of sampled ponds might introduce some uncertainty in the data interpretation and that the results

hence should be handled with care. It is furthermore unknown to what extent MPs are lost in other parts of the stormwater drainage systems, such as deposition in gully pots that are regularly emptied or accumulated in the soil of permeable surfaces such as ditches and infiltration trenches. Therefore, the MPs accumulated in the sediments of the ponds can only to a limited extent reflect the MP abundance in the runoff. Despite these potential biases, the present study still found a strong correlation between the MP abundance in the sediments and the pond hydraulic loading (P-values for both particle number and mass concentration < 0.005), yielding a reasonable confidence in the found correlation.

The sediment MP concentrations showed no correlation with the land use of their catchment, since the least and the most contaminated sediments were both from ponds serving industrial catchments, and the three residential ponds also had MP

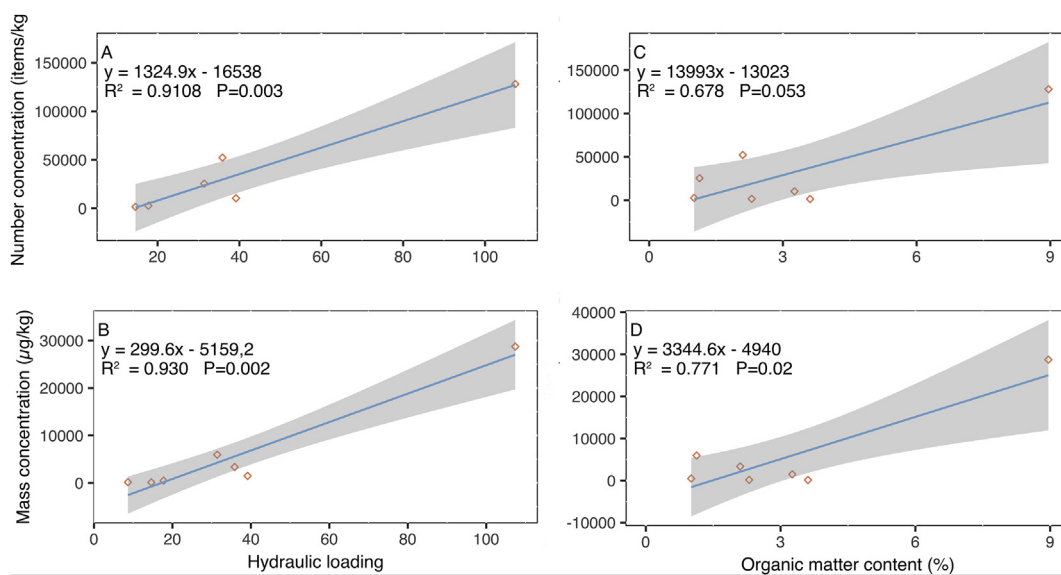


**Fig. 2.** The relationship between MP abundance and the pond hydraulic loading (left), and the sediment organic matter content (right). The MP abundance are presented both as particle number concentration (up) and mass concentration. The solid blue line represents the regression line. The confidence intervals (95%) are highlighted as grey areas. Both the regression, the coefficient of determination (R<sup>2</sup>), and the significance level (P) were presented. (For interpretation of the references to colour in this figure legend, the reader is referred to the Web version of this article.)

accumulation varying with one order of magnitude (Table S1). This is in contrast with the findings of Liu et al. (2019b), who concluded that such correlation did exist for the water phase of the same seven ponds. Other freshwater-related studies reported that population density probably affected the MP pollution level in China's largest inland lake (Xiong et al., 2018), and for Laurentian Great Lakes of the United States, the urbanization level also correlated with the MP pollution (Eriksen et al., 2013).

### 3.4. Polymer composition, size, mass and shape

Analysis using MPhunter (Liu et al., 2019b) enabled MPs to be assigned to one of the following material groups: PE, PS, PVC, PP, PA, PU, polyester, ABS, epoxy, acrylic, SAN, vinyl copolymer, EVA, PVAC, polycarbonate, phenoxy resin, EPDM, acrylic paint, PU paint, and alkyd. Some of these polymers were not commonly detected and hence were gathered into a group of 'others' (ABS, epoxy, SAN, vinyl copolymer, EVA, PVAC, polycarbonate, phenoxy resin, EPDM, alkyd), which contained 70 items in total. Furthermore, acrylic paint (17 items) and PU paint (9 items) were grouped with acrylic and PU, respectively (Table S2).

PP clearly dominated in the ponds, in terms of both number and mass of particles (Fig. 3). When sorted by particle mass, PS ranked as the second most abundant polymer, followed by polyester, PE, PU, PVC, others, and PA. However, when sorted by number of particles PA was the second most abundant polymer, followed by polyester, PE, PS, PU, acrylic, others, and PVC. The high contribution of polymers with low densities indicated that, particle density was not the only factor determining MP sedimentation. But whether this was a result of these materials simply being more abundant, an increased density due to the formation of biofilms on the particles, or a combination of various other factors cannot be determined by the present study (Eerkes-Medrano et al., 2015; Rummel et al., 2017).

Polymer density and particle size had a significant impact on the abundance when comparing number versus mass of particles. For instance, even though PVC was present at low numbers, its mass exceeded that of PA and acrylic due to its higher density. Another pronounced example is PA, which had the second highest number concentration, but as the particle size was the smallest of the polymers (Fig. S3B), it had the lowest mass concentration (Fig. 3).

The polymer composition of the seven ponds analysed was comparable with results from other studies of freshwater sediments. For example, Thompson et al. (2004) find that acrylic, alkyd, PP, PE, PA (nylon), polyester, polymethylacrylate, poly (ethylene:

propylene), and polyvinyl-alcohol were conclusively identified in estuarine and sub-tidal sediments around Plymouth, UK. Polyester was also commonly detected in river sediments in Shanghai (Peng et al., 2018), and PP, PE, and PS were commonly found in river sediments in Portugal (Rodrigues et al., 2018) as well as lake sediments in India (Sruthy and Ramasamy, 2017).

Low-density polymers (PP, PE) accounted for 65.2% by mass and 46.4% by the number of MPs identified overall (Fig. 3). Their abundance in the sediments of the stormwater ponds, as well as in many other sediment types previously reported (Klein et al., 2015; Haave et al., 2019), suggests that density is not the only factor that affects the distribution of polymers between water and sediments. Simple sedimentation in calm water is not sufficient to explain MP retention mechanisms. Other processes related to in-pond hydraulics, turbulence, and sediment organic matter may also have impacted the distribution (Thompson et al., 2004; Nel et al., 2017), as could aggregation with other particles, biofilm growth, and animal uptake (Besseling et al., 2017).

The polymer composition varied significantly between ponds (Fig. S2). For example, PVC was present in comparable concentrations in the residential ponds (R1, R2, R3) and highway pond H1, but it was rarely detected in commercial pond C1 and not detected at all in industrial pond I1. Beyond this, ponds serving the same catchment type did not hold similar distributions of polymers. PP dominated in industrial pond I2, but constituted a much smaller fraction of MPs found in I1. Among the residential ponds, polyester dominated in R1, but PP was the most abundant polymer in R2. These results are in contrast with previous findings for the water phase of the same seven ponds. The water phase of the ponds serving residential and highway catchment, as well as the ones serving industrial and commercial catchments both had similar polymer distribution patterns (Liu et al., 2019b). The reason here fore is unclear, but could be related to the fact that water phase concentrations represent short term MP concentration in the runoff, while the sediments reflect accumulation over several years.

Stormwater retention ponds are physically close to the MP source and receive surface runoff from a well-defined drainage area. It hence seems reasonable to assume that their sediments reflect the MP sources in the drainage area. A similar argument has been brought forward by Rochman (2018), who states that compared with the open ocean, MPs in freshwater and terrestrial systems more readily reveal their original sources, because they are direct receivers of treated and untreated urban, industrial, and agricultural waste. In line with this argument, it seems reasonable to believe that at least some of the MPs found in stormwater ponds originate from the structures and activities in the catchment. However, it cannot be excluded that some of the MPs found in the ponds originated outside the pond drainage area, and had been transported into it by atmospheric deposition (Free et al., 2014). Hence the fact that PP was abundant in all sediments could be due to its use in the drainage area, or it could simply be a consequence of the fact that it is one of the most widely used polymers (PlasticsEurope, 2018), and hence is abundant in atmospheric particles and deposited during dry and wet weather.

When grouping the MPs from all seven ponds into polymer types, there was a clear trend of the median particle size of the polymers:

PVC > PP > others > acrylic > PS > PE > polyester > PU > PA (Fig. S3, Table S2). This trend held almost true also for particle mass, except that acrylic and 'others' switched place in the ranking. When the MPs were grouped by ponds, there was also a trend in the particle size: R1 > I2 > R2 > I1 > C1 > R3 > H1 (Fig. S3, Table S3). This trend, though, did not correlate with land use, and was also in contrast with the findings of the pond water of the same seven ponds (Liu et al., 2019b). MP mass in the ponds also followed this trend, except that R2 had lower average particle mass than I1. A

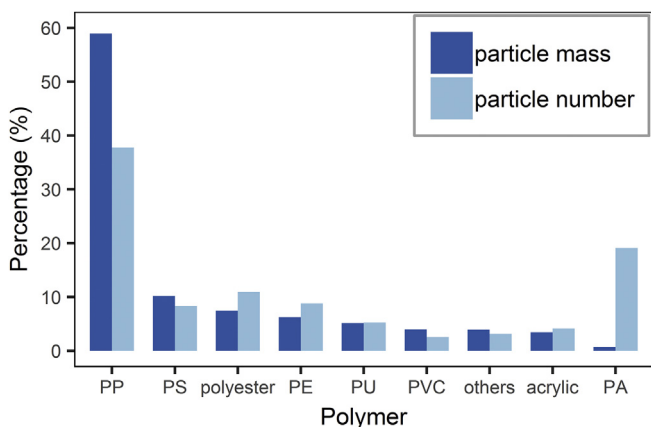


Fig. 3. Polymer composition of the main polymers detected in the seven ponds. The concentration is given as particle mass and number of particles.

likely reason for this slight change is that pond R2 held a relatively higher percentage of PP. PP is the polymer that had the second-largest particle size (Fig. S3), whilst its low density pulled down the average particle mass.

Particles identified by ATR-FTIR were mostly fragments (38 items) followed by film (6 items), whilst only one fiber and one pellet were found (Fig. S4). The majority of the MPs in the smaller size range (10–500 µm) were plump ellipsoids, with the median value of the major to minor dimension ratio at 1.9 (Fig. S6). To compare the shape between polymers, the major dimension was plotted against the minor dimension and fitted to a linear model (Fig. S5). PP particles were found to be the slimmest in shape, where the major dimension on average was close to three times the minor dimension. Although this ratio on its own is not sufficient to determine whether these were truly fibres, it is reasonable to assume that compared to other polymers, PP particles had a higher tendency to be fibres. PU particles were the plumpest in shape, with the major dimension only slightly longer than the minor.

The shape of particles <500 µm in the present study was determined based on the assumption that, all the particles were of ellipsoid shaped (Simon et al., 2018; Liu et al., 2019b). This assumption is a simplification made to allow mass estimation, and the shape information only used for comparison between the polymer types within this study. The shape of particles >500 µm was an actual measurement by the stereomicroscope, and this fraction can hence be compared with other studies. So did for example Sruthy and Ramasamy (2017) – in contrast to the present study – found that film and foam shapes dominated in sediment of Vembanad Lake in India, whilst fibres were the most common shape in Taihu Lake, China (Su et al., 2016). However, it is rather complex to distinguish which specific factors drove the difference in MP shape distribution, as it is a result of a combination of a multitude of anthropogenic activities and environmental processes.

Several important questions remain largely unanswered: What causes the variation in particle shape and how it depends on polymer types? What explains the variation in particle sizes in between polymers and ponds? and within the same stormwater retention pond, what causes the difference in polymer composition between the water phase and the sediment phase? While this first study on MPs in the sediments of stormwater retention ponds raises at least as many questions as it answers, the results are an important step towards a better understanding of MPs in urban and highway runoff and the role of the retention ponds, which mitigating MP pollution from downstream by retain them in sediments.

#### 4. Conclusion

This study is the first evaluation of MPs in the sediments of stormwater retention ponds. It shows that microplastics, and especially small particles (10–250 µm) were prevalent in these sediments. The variation in MP abundance, size distribution, and polymer composition between the ponds was large. Hydraulic loading was an explanatory factor for the difference in MP abundance, while other potential explanations such as land use and sediment organic matter content were not supported. Furthermore, the determination of whether or not stormwater ponds are efficient for controlling overall plastic pollution from urban and highway areas remains a question for future research. It does, though, seem clear that stormwater pond sediments do retain MPs and hence plays a role in managing MPs from urban and highway areas.

#### Acknowledgement

Fan Liu was sponsored by the China Scholarship Council [CSC

NO. 201507000057]. The study was partly funded by the Danish Environmental Protection Agency, Pesticide Research Programme, MST-667-00227. Furthermore, this work resulted from the BONUS CleanWater project was supported by BONUS (Art 185), funded jointly by the EU and Innovation Fund Denmark.

#### Appendix A. Supplementary data

Supplementary data to this article can be found online at <https://doi.org/10.1016/j.envpol.2019.113335>.

#### References

- Andrady, A.L., 2017. The plastic in microplastics: a review. *Mar. Pollut. Bull.* 119 (1), 12–22. <https://doi.org/10.1016/j.marpolbul.2017.01.082>.
- Auta, H.S., Emenike, C.U., Fauziah, S.H., 2017. Distribution and importance of microplastics in the marine environment: A review of the sources, fate, effects, and potential solutions. *Environ. Int.* 102, 165–176. <https://doi.org/10.1016/j.envint.2017.02.013>.
- Abidli, S., Antunes, J.C., Ferreira, J.L., Lahbib, Y., Sobral, P., Trigui El Menif, N., 2018. Microplastics in sediments from the littoral zone of the north Tunisian coast (Mediterranean Sea). *Estuar. Coast. Shelf Sci.* 205, 1–9. <https://doi.org/10.1016/j.ecss.2018.03.006>.
- Allen, S., Allen, D., Phoenix, V.R., Le Roux, G., Durántez Jiménez, P., Simonneau, A., Binet, S., Galop, D., 2019. Atmospheric transport and deposition of microplastics in a remote mountain catchment. *Nat. Geosci.* 12, 339–344. <https://doi.org/10.1038/s41561-019-0335-5>.
- Bentzen, T., Larsen, T., Rasmussen, M., 2009. Predictions of resuspension of highway detention pond deposits in interrain event periods due to wind-induced currents and waves. *J. Environ. Eng.* 135, 1286–1293. [https://doi.org/10.1061/\(asce\)ee.1943-7870.0000108](https://doi.org/10.1061/(asce)ee.1943-7870.0000108).
- Besseling, E., Quik, J.T.K., Sun, M., Koelmans, A.A., 2017. Fate of nano- and microplastic in freshwater systems: a modeling study. *Environ. Pollut.* 220, 540–548. <https://doi.org/10.1016/j.envpol.2016.10.001>.
- Cabernard, L., Roscher, L., Lorenz, C., Gerdt, G., Primpke, S., 2018. Comparison of Raman and Fourier transform infrared spectroscopy for the quantification of microplastics in the aquatic environment. *Environ. Sci. Technol.* 52, 13279–13288. <https://doi.org/10.1021/acs.est.8b03438>.
- Damrat, M., Zaboraska, A., Zajaczkowski, M., 2013. Sedimentation from suspension and sediment accumulation rate in the River Vistula prodelta, Gulf of Gdańsk (Baltic sea). *Oceanologia* 55, 937–950. <https://doi.org/10.5697/oc.55-4.937>.
- Dris, R., Gasperi, J., Mirande, C., Mandin, C., Guerrouache, M., Langlois, V., Tassin, B., 2017. A first overview of textile fibers, including microplastics, in indoor and outdoor environments. *Environ. Pollut.* 221, 453–458. <https://doi.org/10.1016/j.envpol.2016.12.013>.
- Da Costa, J.P., Nunes, A.R., Santos, P.S.M., Girão, A.V., Duarte, A.C., Rocha-Santos, T., 2018. Degradation of polyethylene microplastics in seawater: insights into the environmental degradation of polymers. *J. Environ. Sci. Heal. Part A Toxic Hazard. Substain. Environ. Eng.* 53, 866–875. <https://doi.org/10.1080/10934529.2018.1455381>.
- Di, M., Wang, J., 2018. Microplastics in surface waters and sediments of the three Gorges Reservoir, China. *Sci. Total Environ.* 616–617, 1620–1627. <https://doi.org/10.1016/j.scitotenv.2017.10.150>.
- Eriksen, M., Mason, S., Wilson, S., Box, C., Zellers, A., Edwards, W., Farley, H., Amato, S., 2013. Microplastic pollution in the surface waters of the Laurentian Great lakes. *Mar. Pollut. Bull.* 77, 177–182. <https://doi.org/10.1016/j.marpolbul.2013.10.007>.
- Eerkes-Medrano, D., Thompson, R.C., Aldridge, D.C., 2015. Review microplastics in freshwater systems: a review of the emerging threats, identification of knowledge gaps and prioritisation of research needs. *Water Res.* 75, 63–82. <https://doi.org/10.1016/j.watres.2015.02.012>.
- Free, C.M., Jensen, O.P., Mason, S.A., Eriksen, M., Williamson, N.J., Boldgiv, B., 2014. High-levels of microplastic pollution in a large, remote, mountain lake. *Mar. Pollut. Bull.* 85, 156–163. <https://doi.org/10.1016/j.marpolbul.2014.06.001>.
- Hvitved-Jacobsen, T., Vollertsen, J., Nielsen, A.H., 2010. *Urban and Highway Stormwater Pollution: Concepts and Engineering*. CRC Press, Taylor & Francis Group.
- Hidalgo-Ruz, V., Gutow, L., Thompson, R.C., Thiel, M., 2012. Microplastics in the marine environment: a review of the methods used for identification and quantification. *Environ. Sci. Technol.* 46, 3060–3075. <https://doi.org/10.1021/es2031505>.
- Horton, A.A., Svendsen, C., Williams, R.J., Spurgeon, D.J., Lahive, E., 2017. Large microplastic particles in sediments of tributaries of the River Thames, UK – abundance, sources and methods for effective quantification. *Mar. Pollut. Bull.* 114, 218–226. <https://doi.org/10.1016/j.marpolbul.2016.09.004>.
- Hurley, R.R., Lusher, A.L., Olsen, M., Nizzetto, L., 2018. Validation of a method for extracting microplastics from complex, organic-rich, environmental matrices. *Environ. Sci. Technol.* 52, 7409–7417. <https://doi.org/10.1021/acs.est.8b01517>.
- Hahladakis, J.N., Velis, C.A., Weber, R., Iacovidou, E., Purnell, P., 2018. An overview of chemical additives present in plastics: migration, release, fate and environmental impact during their use, disposal and recycling. *J. Hazard. Mater.* 344,

- 179–199. <https://doi.org/10.1016/j.jhazmat.2017.10.014>.
- Harrison, J.P., Hoellein, T.J., Sapp, M., Tagg, A.S., 2018. Microplastic-associated Biofilms: a Comparison of Freshwater and Marine Environments. *Freshwater Microplastics*. Springer, Cham, pp. 181–201. <https://doi.org/10.1007/978-3-319-61615-5>.
- Haave, M., Lorenz, C., Primpke, S., Gerdt, G., 2019. Different stories told by small and large microplastics in sediment - first report of microplastic concentrations in an urban recipient in Norway. *Mar. Pollut. Bull.* 141, 501–513. <https://doi.org/10.1016/j.marpolbul.2019.02.015>.
- Hartmann, N.B., Hüffer, T., Thompson, R.C., Hassellöv, M., Verschoor, A., Daugaard, A.E., Rist, S., Karlsson, T., Brennholt, N., Cole, M., Herrling, M.P., Hess, M.C., Ivleva, N.P., Lusher, A.L., Wagner, M., 2019. Are we speaking the same language? Recommendations for a definition and categorization framework for plastic debris. *Environ. Sci. Technol.* 53, 1039–1047. <https://doi.org/10.1021/acs.est.8b05297>.
- Jambeck, J.R., Geyer, R., Wilcox, C., Siegler, T.R., Perryman, M., Andrady, A., Narayan, R., Law, K.L., 2015. Plastic waste inputs from land into the ocean. *Science* 347 (6223), 768–771. <https://doi.org/10.1126/science.1260352>.
- Klein, S., Worch, E., Knepper, T.P., 2015. Occurrence and spatial distribution of microplastics in river shore sediments of the rhine-main area in Germany. *Environ. Sci. Technol.* 49, 6070–6076. <https://doi.org/10.1021/acs.est.5b0049>.
- Kole, P.J., Löhr, A.J., Van Belleghem, F.G.A.J., Ragas, A.M.J., 2017. Wear and tear of tyres: a stealthy source of microplastics in the environment. *Int. J. Environ. Res. Public Health* 14 (10), 1265. <https://doi.org/10.3390/ijerph14101265>.
- Kooi, M., Besseling, E., Kroeze, C., van Wezel, A.P., Koelmans, A.A., 2018. Modeling the fate and transport of plastic debris in freshwaters: review and guidance. In: Wagner, M., Lambert, S. (Eds.), *Freshwater Microplastics: Emerging Environmental Contaminants?* Springer International Publishing, Cham, pp. 125–152. [https://doi.org/10.1007/978-3-319-61615-5\\_7](https://doi.org/10.1007/978-3-319-61615-5_7).
- Koelmans, A.A., Mohamed Nor, N.H., Hermesen, E., Kooi, M., Mintenig, S.M., De France, J., 2019. Microplastics in freshwaters and drinking water: critical review and assessment of data quality. *Water Res.* 155, 410–422. <https://doi.org/10.1016/j.watres.2019.02.054>.
- Leslie, H.A., Brandsma, S.H., Van Velzen, M.J.M., Vethaak, A.D., 2017. Microplastics en route: field measurements in the Dutch river delta and Amsterdam canals, wastewater treatment plants, North Sea sediments and biota. *Environ. Int.* 101, 133–142. <https://doi.org/10.1016/j.envint.2017.01.018>.
- Löder, M.G.J., Imhof, H.K., Ladehoff, M., Löschel, L.A., Lorenz, C., Mintenig, S., Piehl, S., Primpke, S., Schrank, I., Laforsch, C., Gerdt, G., 2017. Enzymatic purification of microplastics in environmental samples. *Environ. Sci. Technol.* 51, 14283–14292. <https://doi.org/10.1021/acs.est.7b03055>.
- Liu, F., Nielsen, A.H., Vollertsen, J., 2019a. Sorption and degradation potential of pharmaceuticals in sediments from a stormwater retention pond. *Water* 11, 526. <https://doi.org/10.3390/w11030526>.
- Liu, F., Olesen, K.B., Borregaard, A.R., Vollertsen, J., 2019b. Microplastics in urban and highway stormwater retention ponds. *Sci. Total Environ.* 671, 992–1000. <https://doi.org/10.1016/j.scitotenv.2019.03.416>.
- McCormick, A., Hoellein, T.J., Mason, S.A., Schluep, J., Kelly, J.J., 2014. Microplastic is an abundant and distinct microbial habitat in an urban river. *Environ. Sci. Technol.* 48, 11863–11871. <https://doi.org/10.1021/es503610r>.
- Masura, J., Baker, J., Foster, G., Arthur, C., Herring, C., 2015. *Laboratory Methods for the Analysis of Microplastics in the Marine Environment: Recommendations for Quantifying Synthetic Particles in Waters and Sediments*. NOAA. Technical Memorandum NOS-OR&R-48.
- Minelgaite, G., Nielsen, A.H., Pedersen, M.L., Vollertsen, J., 2017. Photodegradation of three stormwater biocides. *Urban Water J.* 14, 53–60. <https://doi.org/10.1080/1573062X.2015.1076489>.
- Mintenig, S.M., Int-Veen, I., Löder, M.G.J., Primpke, S., Gerdt, G., 2017. Identification of microplastic in effluents of waste water treatment plants using focal plane array-based micro-Fourier-transform infrared imaging. *Water Res.* 108, 365–372. <https://doi.org/10.1016/j.watres.2016.11.015>.
- Nel, H.A., Dalu, T., Wasserman, R.J., 2017. Sinks and sources: assessing microplastic abundance in river sediment and deposit feeders in an Austral temperate urban river system. *Sci. Total Environ.* 612, 950–956. <https://doi.org/10.1016/j.scitotenv.2017.08.298>.
- Olesen, K.B., Stephansen, D.A., Alst, N. Van, Vollertsen, J., 2019. Microplastics in a stormwater pond. *Water* 11, 1466. <https://doi.org/10.3390/w11071466>.
- Primpke, S., Lorenz, C., Rascher-Friesenhausen, R., Gerdt, G., 2017. An automated approach for microplastics analysis using focal plane array (FPA) FTIR microscopy and image analysis. *Anal. Methods* 9, 1499–1511. <https://doi.org/10.1039/c6ay02476a>.
- Peng, G., Xu, P., Zhu, B., Bai, M., Li, D., 2018. Microplastics in freshwater river sediments in Shanghai, China: a case study of risk assessment in mega-cities. *Environ. Pollut.* 234, 448–456. <https://doi.org/10.1016/j.envpol.2017.11.034>.
- PlasticsEurope, 2018. *Plastics-the Facts 2018*. Brussels.
- Primpke, S., Wirth, M., Lorenz, C., Gerdt, G., 2018. Reference database design for the automated analysis of microplastic samples based on Fourier transform infrared (FTIR) spectroscopy. *Anal. Bioanal. Chem.* 410, 5131–5141. <https://doi.org/10.1007/s00216>.
- Rummel, C.D., Jahnke, A., Gorokhova, E., Kühnel, D., Schmitt-Jansen, M., 2017. Impacts of biofilm formation on the fate and potential effects of microplastic in the aquatic environment. *Environ. Sci. Technol. Lett.* <https://doi.org/10.1021/acs.estlett.7b00164>.
- Rochman, C.M., 2018. Microplastics research-from sink to source. *Science* 360 (6384), 28–29. <https://doi.org/10.1126/science.aar7734>.
- Rodrigues, M.O., Abrantes, N., Gonçalves, F.J.M., Nogueira, H., Marques, J.C., Gonçalves, A.M.M., 2018. Spatial and temporal distribution of microplastics in water and sediments of a freshwater system (Antuã River, Portugal). *Sci. Total Environ.* 633, 1549–1559. <https://doi.org/10.1016/j.scitotenv.2018.03.233>.
- Szmytkiewicz, A., Zalewska, T., 2014. Sediment deposition and accumulation rates determined by sediment trap and <sup>210</sup>Pb isotope methods in the Outer Puck Bay (Baltic Sea). *Oceanologia* 56, 85–106. <https://doi.org/10.5697/oc.56-1.085>.
- Su, L., Xue, Y., Li, L., Yang, D., Kolandhasamy, P., Li, D., Shi, H., 2016. Microplastics in Taihu Lake, China. *Environ. Pollut.* 216, 711–719. <https://doi.org/10.1016/j.envpol.2016.06.036>.
- Sruthy, S., Ramasamy, E.V., 2017. Microplastic pollution in Vembanad Lake, Kerala, India: the first report of microplastics in lake and estuarine sediments in India. *Environ. Pollut.* 222, 315–322. <https://doi.org/10.1016/j.envpol.2016.12.038>.
- Scheurer, M., Bigalke, M., 2018. Microplastics in Swiss floodplain soils. *Environ. Sci. Technol.* 52, 3591–3598. <https://doi.org/10.1021/acs.est.7b06003>.
- Simon, M., Van Alst, N., Vollertsen, J., 2018. Quantification of microplastic mass and removal rates at wastewater treatment plants applying Focal Plane Array (FPA)-based Fourier Transform Infrared (FTIR) imaging. *Water Res.* 142, 1–9. <https://doi.org/10.1016/j.watres.2018.05.019>.
- Thompson, R.C., Olsen, Y., Mitchell, R.P., Davis, A., Rowland, S.J., John, A.W.G., McGonigle, D., Russell, A.E., 2004. Lost at sea: where is all the plastic? *Science* 304 (5672), 838. <https://doi.org/10.1126/science.1094559>.
- Talvitie, J., Mikola, A., Setälä, O., Heinonen, M., Koistinen, A., 2017. How well is microlitter purified from wastewater? A detailed study on the stepwise removal of microlitter in a tertiary level wastewater treatment plant. *Water Res.* 109, 164–172. <https://doi.org/10.1016/j.watres.2016.11.046>.
- Velzeboer, I., Kwadijk, C.J.A.F., Koelmans, A.A., 2014. Strong sorption of PCBs to nanoplastics, microplastics, carbon nanotubes, and fullerenes. *Environ. Sci. Technol.* 48, 4869–4876. <https://doi.org/10.1021/es405721v>.
- Van Cauwenberghhe, L., Devriese, L., Galgani, F., Robbens, J., Janssen, C.R., 2015. Microplastics in sediments: a review of techniques, occurrence and effects. *Mar. Environ. Res.* 111, 5–17. <https://doi.org/10.1016/j.marenvres.2015.06.007>.
- Vaughan, R., Turner, S.D., Rose, N.L., 2017. Microplastics in the sediments of a UK urban lake. *Environ. Pollut.* 229, 10–18. <https://doi.org/10.1016/j.envpol.2017.05.057>.
- Woodall, L.C., Sanchez-Vidal, A., Canals, M., Paterson, G.L.J., Coppock, R., Sleight, V., Calafat, A., Rogers, A.D., Narayanaswamy, B.E., Thompson, R.C., 2014. The deep sea is a major sink for microplastic debris. *R. Soc. Open Sci.* 1 (4), 140317–140317. <https://doi.org/10.1098/rsos.140317>.
- Wang, J., Peng, J., Tan, Z., Gao, Y., Zhan, Z., Chen, Q., Cai, L., 2017. Microplastics in the surface sediments from the Beijing River littoral zone: composition, abundance, surface textures and interaction with heavy metals m-FTIR. *Chemosphere* 171, 248–258. <https://doi.org/10.1016/j.chemosphere.2016.12.074>.
- Wang, Z., Su, B., Xu, X., Di, D., Huang, H., Mei, K., Dahlgren, R.A., Zhang, M., Shang, X., 2018. Preferential accumulation of small (<300 Mm) microplastics in the sediments of a coastal plain river network in eastern China. *Water Res.* 144, 393–401. <https://doi.org/10.1016/j.watres.2018.07.050>.
- Windsor, F.M., Durance, I., Horton, A.A., Thompson, R.C., Tyler, C.R., Ormerod, S.J., 2019. A catchment-scale perspective of plastic pollution. *Glob. Chang. Biol.* 25 (4), 1207–1221. <https://doi.org/10.1111/gcb.14572>.
- Xiong, X., Zhang, K., Chen, X., Shi, H., Luo, Z., Wu, C., 2018. Sources and distribution of microplastics in China's largest inland lake – Qinghai Lake. *Environ. Pollut.* 235, 899–906. <https://doi.org/10.1016/j.envpol.2017.12.081>.
- Yang, L., Li, K., Cui, S., Kang, Y., An, L., Lei, K., 2019. Removal of microplastics in municipal sewage from China's largest water reclamation plant. *Water Res.* 175–181. <https://doi.org/10.1016/j.watres.2019.02.046>.
- Zhan, F., Zhang, H., Wang, J., Xu, J., Yuan, H., Gao, Y., Su, F., Chen, J., 2017. Release and gas-particle partitioning behaviors of short-chain chlorinated paraffins (SCCPs) during the thermal treatment of polyvinyl chloride flooring. *Environ. Sci. Technol.* 51, 9005–9012. <https://doi.org/10.1021/acs.est.7b01965>.
- Zhang, G.S., Liu, Y.F., 2018. The distribution of microplastics in soil aggregate fractions in southwestern China. *Sci. Total Environ.* 642, 12–20. <https://doi.org/10.1016/j.scitotenv.2018.06.004>.